Supporting Information

Effect of dye coverage on performance in dye-sensitized solar cells with cobalt-based electrolyte

Meysam Pazoki[†,‡], Peter William Lohse[†], Nima Taghavinia[‡*], Anders Hagfeldt[†] and Gerrit Boschloo[†*]

S1. Calculation of amount of adsorbed dye and Langmuir isotherm

The dye coverage in the terms of mol per square centimeter of dyed film was obtained from optical absorption data of dyes films (Figure 1) using the formula $A=1000\varepsilon\Gamma$ (ref S1), where **A** is the absorbance, ε is molar extinction coefficient (M^{-1} cm^{-1}) and Γ (mol cm^{-2}) the dye coverage on the film. The value of ε (17 000 M^{-1} cm^{-1} at 450 nm) was adopted from ref. S2.

The Langmuir adsorption isotherm can be written as $\Gamma = \Gamma_{max}KC/(1+KC)$, with K the binding constant for adsorption, Γ_{max} the maximum load on TiO_2, and C is the dye concentration in the dye bath.

Γ_{max} was determined to 1.2×10^{-7} mol cm^{-2} for a 5.8 μm thick TiO_2 film. BET analysis gave 61.8 m^2/g and a total pore volume of 0.47 cm^3/g, from which a porosity of 64% is calculated using bulk density of anatase TiO_2 of 3.8 g cm^{-3}. 1 cm^2 of the TiO_2 film consists of $0.36 \times 5.8\times10^{-4} = 2.09\times10^{-4}$ cm^3 pure TiO_2, weighing 0.79 mg, with a surface area of 490 cm^2. Area occupied by a single D35 molecule on TiO_2 is thus: $490\times10^{14} / (1.2\times10^{-7} \times 6.023\times10^{23}) = 0.68$ nm^2.

S2. Q_{SC} as function of Jsc for D35-sensitized solar cells with cobalt-based electrolyte and with different dye load

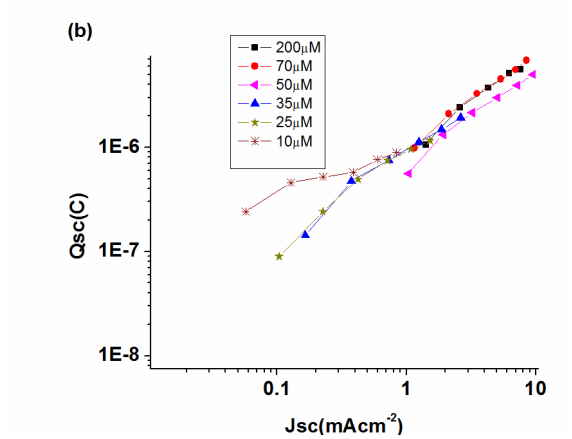

Figure S1. Charge extraction graph of Qsc of DSCs with different dye loading times

S.3 Transient optical spectra of D35 on mesoporous TiO_2

Figure S3 shows the absorption spectra of oxidized D35 dye adsorbed on mesoporous TiO_2 measured by spectroelectrochemistry using a 3 electrode cell configuration. D35 is oxidized at positive applied potential by a hole-hopping mechanism. The TiO_2 film is isolating under these conditions and no Stark effects on the D35 dye molecules are expected.

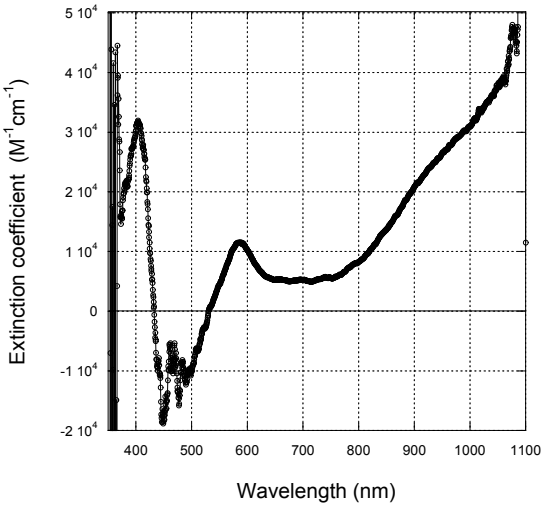

Figure S2. Differential absorption spectrum of oxidized D35 measured by spectroelectrochemistry. (Spectrum oxidized dye minus spectrum ground state dye) Experimental data courtesy of Dr. Ute Cappel.

An electroabsorption spectrum of D35 dye on TiO_2 is shown in Figure S3. Spray pyrolysis was used for fabrication of flat TiO_2 on the FTO. TiO_2 flat layers were immersed in dye bath for 12 hours. 0.5% wt of PMMA in Dichloromethane solution was spin coated on the dyed films (4200 RPM, 30s) and finally 10 nm silver layer was deposited on the top of PMMA by thermal deposition. An AC voltage (2.5-10 V, 93 Hz) was applied on the silver/FTO providing an electric field across the dye. This results in a Stark effect on the adsorbed D35 molecules, changing absorption spectra of D35 dye [ref 27 in main article] and shifting the spectrum to shorter wavelengths when a negative voltage is applied on the TiO_2. We can interpret the absorption bleach at 550 nm as a Stark bleach.

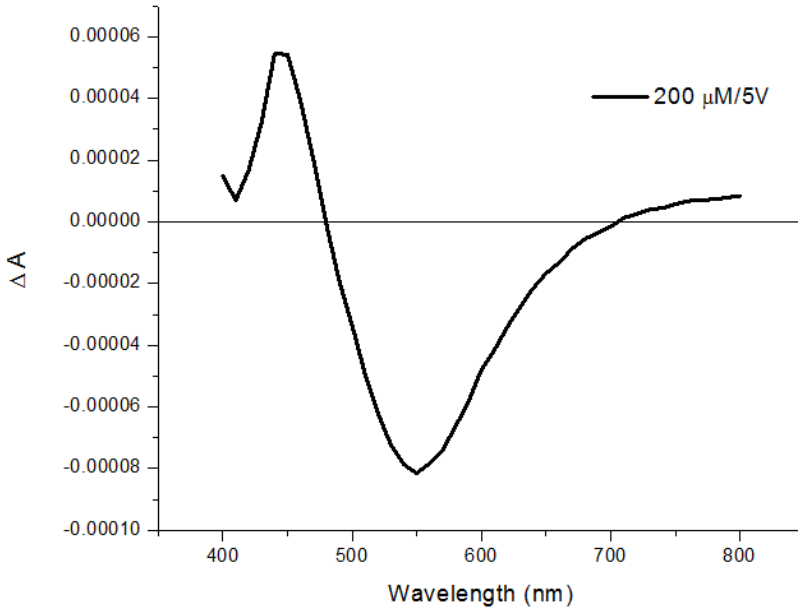

Figure S3 Electroabsorption spectrum of D35 dye adsorbed on flat TiO_2

A photoinduced spectrum of D35 on TiO_2 without electrolyte is shown in Figure S5 in which we can observe the ground state bleach, Stark effect bleach, oxidized dye spectra and absorption of TiO_2 conduction band electrons. Ground state bleach appears near dye absorption maxima (480 nm) and Stark effect bleach for D35 is placed around 550 nm. The long wavelength feature, an increasing absorption is mainly attributed to oxidized D35 dye (compare Fig S5 with Fig. S2); the contribution from electrons in the TiO_2 is small as their extinction coefficient is low (about 1200 $M^{-1}cm^{-1}$). In presence of the cobalt electrolyte, the dye regeneration time (~10

microsecond) is much faster than PIA light modulation frequency (~10 ms) and we can observe efficient regeneration of D35 and negligible amount of oxidized dye (Figure 6 of main article).

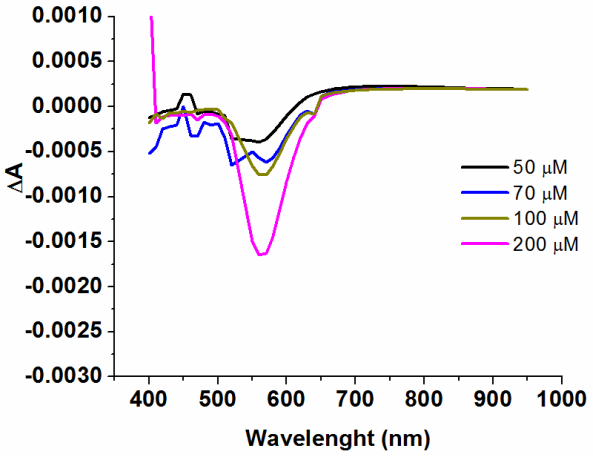

Figure S4 Normalized PIA spectra of DSCs with different dye coverage (same data as Fig. 7). The spectra are normalized to the same electron density in TiO_2.

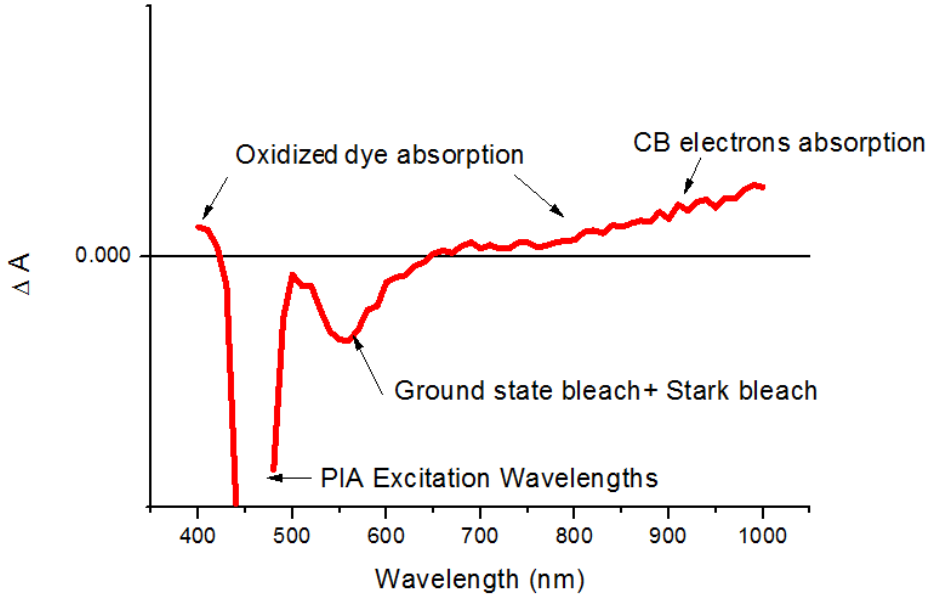

Figure S5. PIA spectrum of D35 on TiO_2 without electrolyte.

S.4 EIS analysis of the cells with different dye coverage

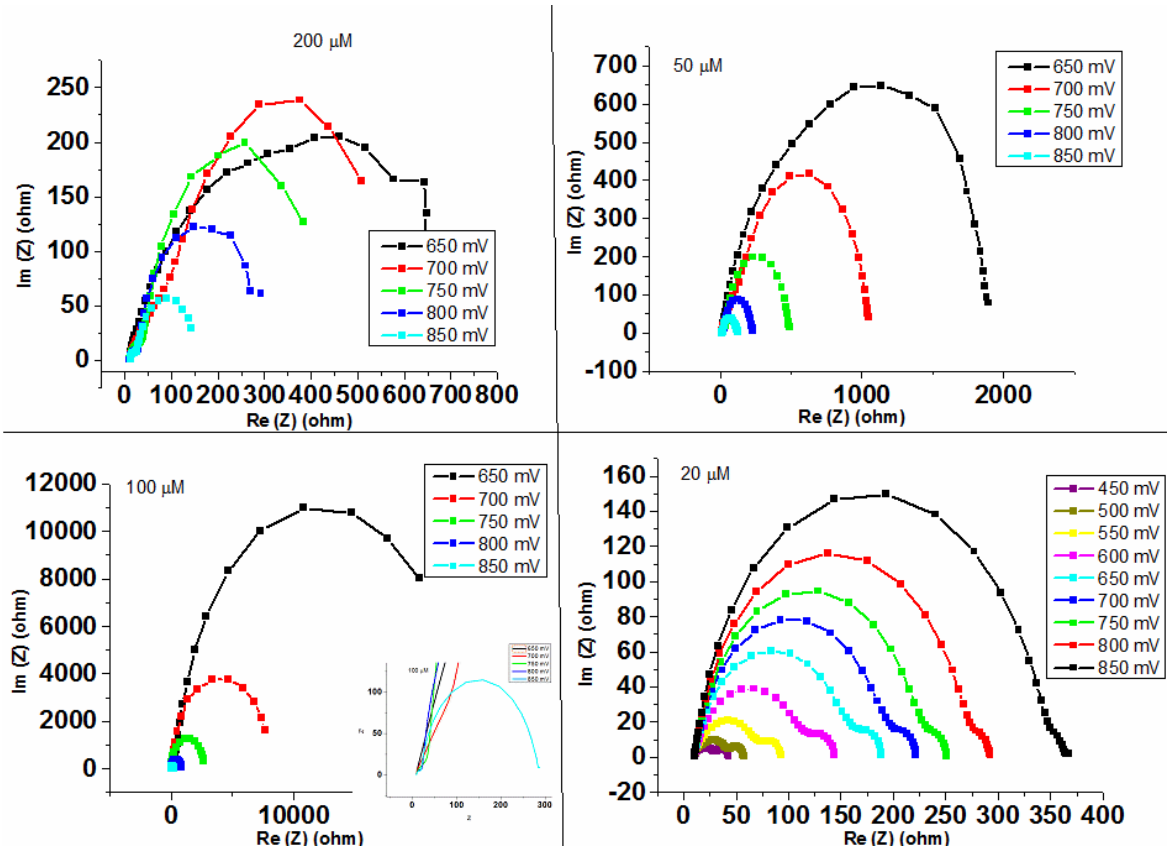

Figure S.6 EIS spectra of theD35-sensitized DSCs with different dye load in the dark at different bias potentials.

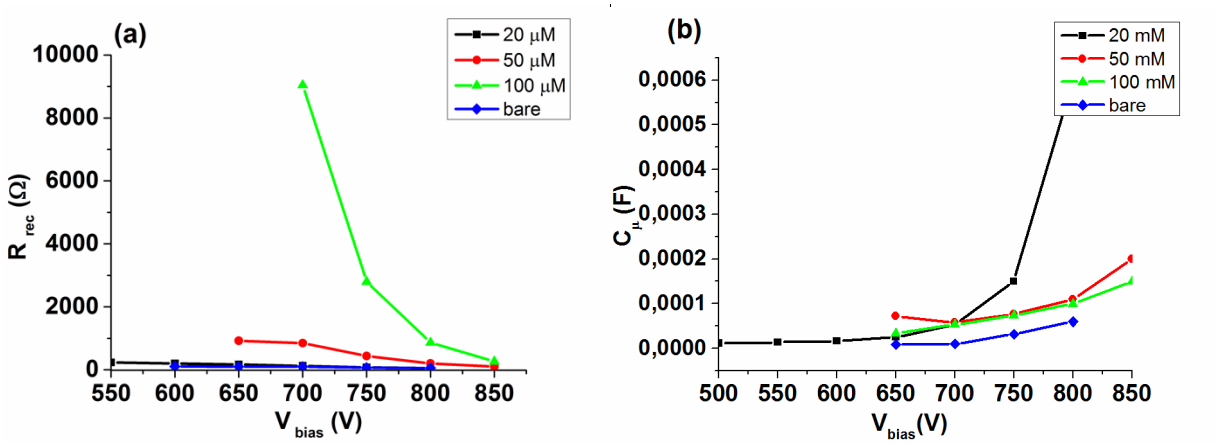

Figure S7. Results from electrochemical impedance spectroscopy of D35-sensitized solar cells with different dye load. (a) Recombination resistance, and (b) chemical capacitance as function of applied forward potential in the dark. A simple capacitor|| resistor model was used to fit the middle arc of the EIS spectrum .

S5. Studying the effect of Li-salt in the dye solution

Working electrodes were dyed in different D35 dye bath solutions: (20 µM in ethanol, 20 µM in 0.1M $LiClO_4$ in ethanol, 100 µM in ethanol , 100 µM in 0.1M $LiClO_4$ at ethanol). The UV/Vis absorption spectra of the dyed electrodes (in air) show almost the same absorption for electrodes of dye bath with/without Li salts (Fig. S8). Presence of Li leads to lower absorbance of the dye and shifting the dye absorption spectra which is indicative of different dye molecule configuration (or environment) on the surface. Current voltage curves and electron lifetime graphs of fabricated solar cells show the same trend of figure 2 and figure 4.a of main article (Table S1 and figure S9). Presence of Li salts inside the solution helps to enhance the current even we have a little bit lower dye adsorption in the case of Li salt based dye bathes.

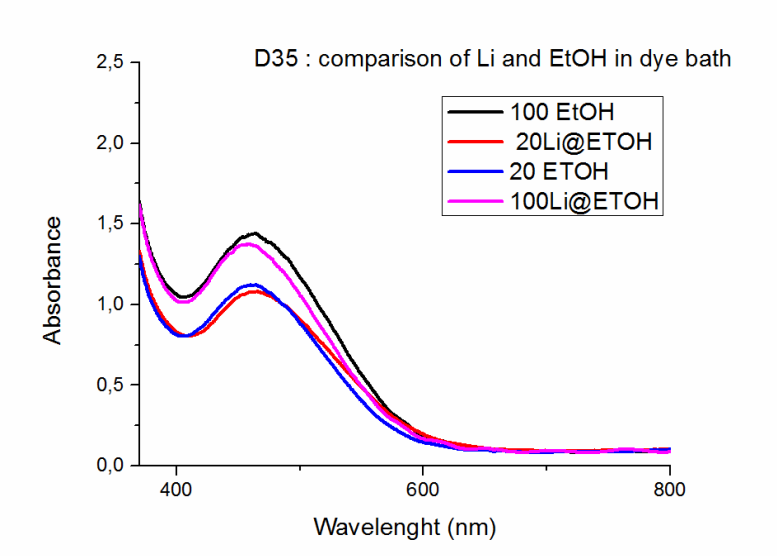

Figure S8. UV/Vis absorption spectra of the sensitized electrodes dyed in ethanolic dye solutions with or without Li salt.

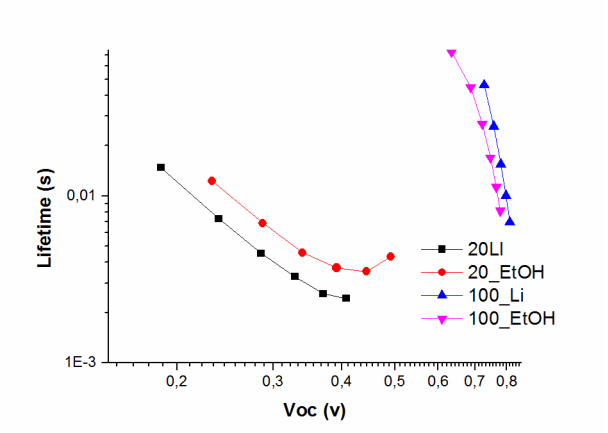

Figure S9. Electron lifetime for DSCs with different dye concentrations with/without Li salt in dye bath.

Table S1. Photon to energy conversion efficiency characteristics of fabricated cells with different dye concentrations with/without Li salt in dye bath.

Cell	Intensity (Wm-2)	Eff (%)	Voc (V)	Jsc (mAcm-2)	FF (%)
100etoh	1000	4.31	0.790	7.99	68.3
100li	1000	5.37	0.825	9.11	71.4
20li	1000	0.796	0.435	3.61	50.
20etoh	1000	0.993	0.495	4.00	50.0

S6. Iodide based DSCs with D35 and Z907 dyes.

In the case of two electron redox mediators of iodide based DSCs, the dye protection against recombination has much less importance. We have studied test cells with iodide electrolyte using D35 or Z907 dyes with 20 and 100 μM dye concentrations in the dye bath. Figure S10 and S11 shows the lifetime and transport time of the fabricated cells with D35 and Z907 dye. There is no evidence for the importance of dye coverage protection against recombination in the data (see also table S2 and S3).

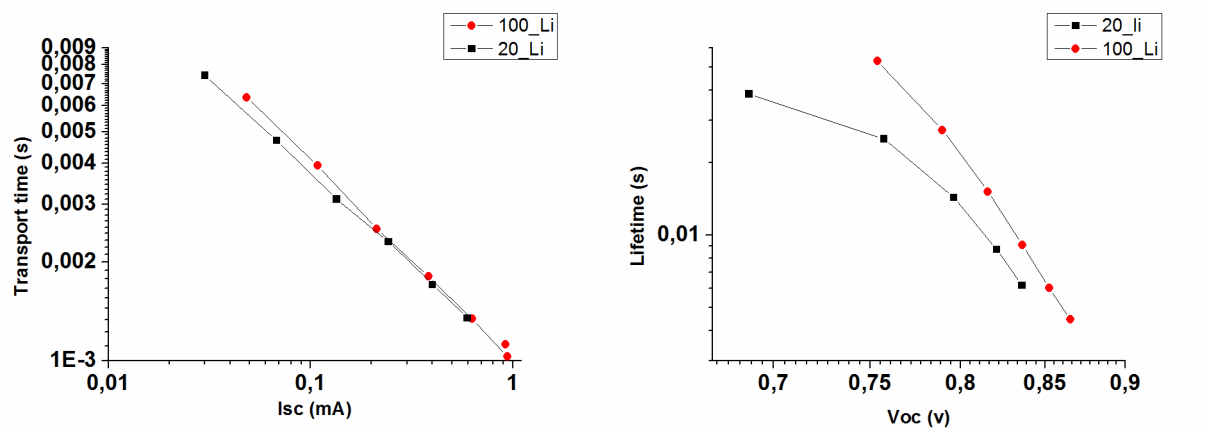

Figure S10. Transport time and lifetime for DSCS with different D35 dye concentrations using iodide electrolyte.

Table S2. Photon to energy conversion efficiency characteristics of fabricated cells with different D35 dye concentrations using iodide electrolyte.

cell	Intensity (Wm-2)	Eff (%)	Voc (V)	Jsc (mAcm-2)	FF
20li	1000	3.03	0.830	5.19	70
100li	1000	3.69	0.855	6,02	71

Figure S11 and table S3 show the data for the DSCs based on iodide electrolyte using Z907 dye with different dye loading concentrations.

Table S3. . Photon to energy conversion efficiency characteristics of fabricated cells with different Z907 dye concentrations using iodide electrolyte.

cell	Intensity (Wm-2)	Eff (%)	Voc (V)	Jsc (mAcm-2)	FF
20li	1000	2.70	7.75	4.55	76.4
100li	1000	3.10	7.70	5.29	76.1

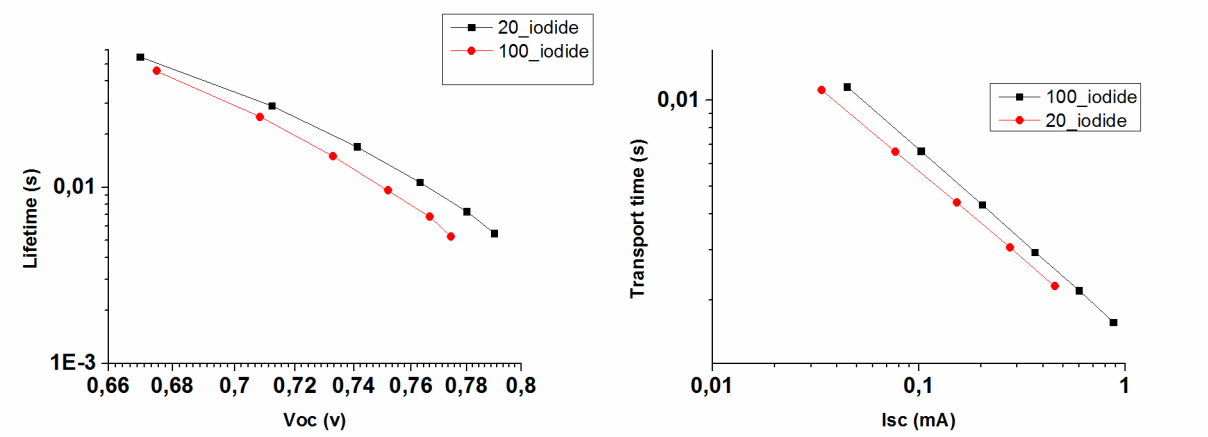

Figure S11. Lifetime and transport time for DSCs with different Z907 dye concentrations using iodide electrolyte.

Table S4. *Fitting parameters for the exponential decay functions of figure 7. The electrodes dyed with different D35 dye concentration solutions and Co(bpy)$_3$-electrolyte was used to regenerate the oxidized dye.*

Dye bath (μM)	A1	τ1(μs)	*A2*	τ2(μs)	*A3*	τ3(μs)
100	0.83	6.81	0.077	34.82	0.045	484.17
80	0.86	7.41	0.126	32.26	0.045	264.29
70	0.85	6.27	0.137	22.35	0.043	443.60
50	0.82	6.76	0.127	26.92	0.041	307.02
35	0.99	5.40	0.218	20.30	0.033	310.98
25	1.04	7.36	0.196	29.59	0.040	329.19
10	0.86	3.49	0.183	17.05	0.093	408.18

References

[S1] Ardo, S. And Meyer, G.J., *J. Am. Chem. Soc.* 2011, 133, 15384

[S2] X. Jiang et al, Adv. Func. Mater 2011, 21, 2944.